Received 19 April 2014
Revised 24 August 2014
18 October 2014
Accepted 18 October 2014

Mixed convection over an inclined wavy surface embedded in a nanofluid saturated porous medium

D. Srinivasacharya and P. Vijay Kumar
Department of Mathematics, National Institute of Technology, Warangal, India

Abstract

Purpose – The purpose of this paper is to study the mixed convection in a nanofluid along an inclined wavy surface embedded in a porous medium.

Design/methodology/approach – The complex wavy surface is transformed to a smooth surface by employing a coordinate transformation. Using the similarity transformation, the governing equations are transformed into a set of ordinary differential equations and then lineralized using the successive linearization method. The Chebyshev pseudo spectral method is then used to solve linearized differential equations.

Findings – The effects of Brownian motion parameter, thermophoresis parameter, amplitude of the wavy surface, angle of inclination of the wavy surface for aiding and opposing flows on the non-dimensional velocity, temperature, nanoparticle volume fraction, heat and nanoparticle mass transfer rates are studied and presented graphically.

Originality/value – This is the first instance in which mixed convection, inclined wavy surface and nanofluid is employed to model fluid flow.

Keywords Porous medium, Inclined wavy surface, Nanofluid, Spectral method

Paper type Research paper

1. Introduction

In recent years, research has been carried out on convective heat transfer in nanofluids due to its wide engineering applications. Choi (1995) is the first person who used the term nanofluids, refer to those fluids in which nanometer sized particles are suspended in conventional heat transfer fluids. Conventional heat transfer fluids such as water and oil are poor heat transfer fluids. So as to improve the thermal conductivity of these fluids, nanosized particles are being suspended in them. Nanofluids are used in the production of nano structured materials for cleaning oil from surfaces due to their exceptional wetting and spreading behavior. Nanofluids are used as coolant in heat exchangers, electronic cooling system (flat plate) and radiators. Nanofluids have many important applications in engineering. To name just a few, this includes microelectronics, microfluidics, high power X-rays, transportation, solid-state lighting, scientific measurement, material processing, biomedical, medical and material synthesis (Das *et al.*, 2007). A detailed review of literature containing enhancement of heat transfer in nanofluids can be found in Xuan and Li (2000) and Kakac and Pramuanjaroenkij (2009).

Convective flows in porous media have been extensively studied in recent years and they have included several physical effects. A detailed review of convective flows in porous media is presented in the books by Nield and Bejan (2006), Ingham and pop (2005) and Vafai (2005). Mixed convective heat and mass transfer problems are used in a wide range of industrial and engineering applications that include heat exchangers,

International Journal of Numerical Methods for Heat & Fluid Flow
Vol. 25 No. 8, 2015
pp. 1774-1792

0961-5539
DOI 10.1108/HFF-04-2014-0104

nuclear reactors, thermal insulation systems, electronic device cooling, oil separation from sand by steam, packed bed chemical reactors, underground disposal of nuclear waste materials and food storage. Convective transport in nanofluids was studied by Buongiorno (2006). Cheng and Minkowycz (1977) and Cheng (1977) were the first to investigate the steady free and mixed convection flow about a vertical impermeable surface in a fluid-saturated porous medium. Later, Merkin (1980) studied the mixed convection boundary layer flow on a vertical surface in a saturated porous medium. Lai (1991) considered the coupled heat and mass transfer by mixed convection from a vertical plate in a saturated porous medium. Chin *et al.*, (2007) studied the effect of variable viscosity on mixed convection boundary layer flow over a vertical impermeable surface embedded in porous medium. It has been found that dual solutions exist and boundary separation occurs in opposing flow. Ahmad and Pop (2010) obtained numerical results for the mixed convection boundary layer flow past a vertical flat plate embedded in a porous medium filled with nanofluids. Guerroudj and Kahalerras (2012) adopted the Brinkman-Forchheimer extended Darcy model with the Boussinesq approximation for the mixed convection in an inclined channel with heated porous blocks. Gorla and Hossain (2013) studied mixed convection boundary layer flow past a vertical cylinder in a porous medium saturated with a nanofluid. Chamkha *et al.* (2014) presented a boundary layer analysis for the mixed convection past a vertical wedge in a porous medium saturated with a power law type non-Newtonian nanofluid. Roşca *et al.* (2014) numerically solved the problem of steady mixed convection boundary layer flow past a vertical flat plate embedded in a fluid-saturated porous medium filled by a nanofluid.

The study of heat transfer from irregular surfaces (wavy surfaces) is a problem of fundamental importance. Irregularities in surfaces occur in many practical situations which enhances the heat transfer characteristics. These irregularities encounter in several heat transfer devices such as microelectronic devices, flat plate solar collectors and flat plate condensers in refrigerators. Moulic and Yao (1989) studied mixed convection along a wavy surface. Hsu *et al.* (2000) considered the study of mixed convection of micro polar fluids along a vertical wavy surface. Jang and Yan (2004) studied the mixed convection heat and mass transfer along a vertical wavy surface. Wang and Chen (2005) obtained numerical results for the problem of mixed convection boundary layer flow on inclined wavy plates including the magnetic field effect. Molla and Hossain (2007) used kellor box method to investigate the problem of radiation effect on mixed convection laminar flow along a vertical wavy surface. It has been revealed that increase in the roughness of the wavy surface enhances the total heat transfer rate. The problem of mixed convection boundary layer flow over a vertical cone embedded in a porous medium saturated with a nanofluid in the presence of thermal radiation was studied by Chamkha *et al.* (2013). Hang *et al.* (2013) analysed the problem of mixed convection flow of a nanofluid in a vertical channel with the Buongiorno mathematical model. Rohni *et al.* (2013) investigated the mixed convection boundary layer flow on a vertical circular cylinder embedded in a porous medium filled with a nanofluid for both cases of heated and cooled cylinder. A numerical simulation of mixed convection flow in a square lid-driven cavity containing porous medium filled with an Al_2O_3 – water nanofluid was studied by Nitesh *et al.* (2013).

Hence, preceding literature survey shows that the mixed convection in a nanofluid along an inclined wavy surface has not been investigated so far. The objective of this study is to obtain the numerical results of mixed convection heat and nanoparticle

mass transfer in a nanofluid along an inclined wavy surface embedded in porous medium. The results are obtained using successive linearization method (SLM). The numerical results include the effect of mixed convection parameter, wavy amplitude, angle of inclination of the wavy surface, Brownian motion parameter, thermophoresis parameter on the non-dimensional velocity, temperature, nanoparticle volume fraction and the heat and nanoparticle mass transfer rates.

2. Mathematical formulation

Consider the steady laminar incompressible two-dimensional boundary layer mixed convection flow along a semi-infinite inclined wavy surface embedded in a nanofluid saturated Darcy porous medium. The wavy plate is inclined at an angle A ($0° \leqslant A \leqslant 90°$) to the horizontal. The coordinate system is shown in Figure. 1. The wavy surface is described by:

$$y = \delta(x) = a \sin\left(\pi x / l\right) \tag{1}$$

where a is the amplitude of the wavy surface, and $2l$ is the characteristic length of the wavy surface. The wavy surface is maintained at constant temperature T_w and constant nanoparticle volume fraction ϕ_w which are higher than the porous medium temperature T_∞ and nanoparticle volume fraction ϕ_∞ sufficiently far from the wavy surface.

We consider the porous medium to be homogeneous and isotropic and is saturated with a fluid which is in local thermodynamic equilibrium with the solid matrix. The fluid has constant properties except the density in the buoyancy term of the balance of momentum equation. Using the Boussinesq approximation, the governing equations for this problem under the laminar boundary layer flow assumptions, and

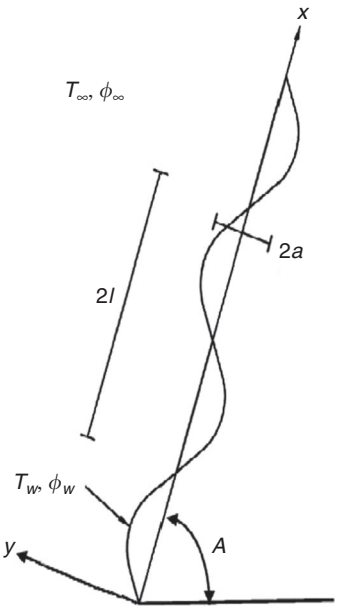

Figure 1.
Physical model

using the Darcy's flow through a homogeneous porous medium near the inclined wavy surface are given by:

$$\frac{\partial u}{\partial x}+\frac{\partial v}{\partial y}=0 \tag{2}$$

$$\frac{\partial u}{\partial y}-\frac{\partial v}{\partial x}=\frac{(1-\phi_\infty)\rho f_\infty \beta K g}{\mu}\left(\frac{\partial T}{\partial y}\sin A-\frac{\partial T}{\partial x}\cos A\right) -\frac{\left(\rho_p-\rho_{f_\infty}\right)Kg}{\mu}\left(\frac{\partial \phi}{\partial y}\sin A-\frac{\partial \phi}{\partial x}\cos A\right) \tag{3}$$

$$u\frac{\partial T}{\partial x}+v\frac{\partial T}{\partial y}=\alpha\left(\frac{\partial^2 T}{\partial x^2}+\frac{\partial^2 T}{\partial y^2}\right)+\gamma\left\{D_B\left(\frac{\partial \phi}{\partial x}\frac{\partial T}{\partial x}+\frac{\partial \phi}{\partial y}\frac{\partial T}{\partial y}\right)+\frac{D_T}{T_\infty}\left[\left(\frac{\partial T}{\partial x}\right)^2+\left(\frac{\partial T}{\partial y}\right)^2\right]\right\} \tag{4}$$

$$u\frac{\partial \phi}{\partial x}+v\frac{\partial \phi}{\partial y}=D_B\left(\frac{\partial^2 \phi}{\partial x^2}+\frac{\partial^2 \phi}{\partial y^2}\right)+\frac{D_T}{T_\infty}\left(\frac{\partial^2 T}{\partial x^2}+\frac{\partial^2 T}{\partial y^2}\right) \tag{5}$$

where u and v are the Darcy velocity components in the x and y directions, respectively, T is the temperature, ϕ is the nanoparticle concentration, g is the acceleration due to gravity, K is the permeability, ρ_f is the density of the base fluid, ρ_p is the density of the particles. α is the effective thermal diffusivity, β is the volumetric thermal expansion coefficient of the nanofluid, μ is the dynamic viscosity of the fluid, D_B is the Brownian diffusion coefficient, D_T is the thermophoretic diffusion coefficient and γ is the ratio between the effective heat capacity of the nanoparticle material and heat capacity of the fluid. The above equations are considered on the assumption that the nanosized particles are suspended in uniform distribution in a base fluid to form a nanofluid. When the nanofluid passes through porous media, the suspension of the nanoparticles is maintained using a surfactant or some surface charge technology to prevent their agglomeration and to avoid being captured by the porous matrix.

The boundary conditions are:

$$v=0, T=T_w, \phi=\phi_w, at\ y=\delta(x) \tag{6a}$$

$$u\to U_\infty, T\to T_\infty, \phi\to\phi_\infty,\ as\ y\to\infty \tag{6b}$$

Now we introduce the stream function ψ by:

$$u=\frac{\partial \psi}{\partial y}, v=-\frac{\partial \psi}{\partial x} \tag{7}$$

and the following non-dimensional variables:

$$\hat{x}=\frac{x}{l},\hat{y}=\frac{y}{l},\hat{a}=\frac{a}{l},\hat{\delta}=\frac{\delta}{l},\theta=\frac{T-T_\infty}{T_w-T_\infty},s=\frac{\phi-\phi_\infty}{\phi_w-\phi_\infty},\hat{\psi}=\frac{\psi}{U_\infty l} \tag{8}$$

In Equations (3)-(5), we get the following system of non-dimensional equations:

$$\frac{\partial^2\hat{\psi}}{\partial x^2}+\frac{\partial^2\hat{\psi}}{\partial y^2}=\frac{Ra}{Pe}\left[\frac{\partial\theta}{\partial\hat{y}}\sin A-\frac{\partial\theta}{\partial\hat{x}}\cos A-N_r\left(\frac{\partial s}{\partial\hat{y}}\sin A-\frac{\partial s}{\partial\hat{x}}\cos A\right)\right] \tag{9}$$

$$\frac{\partial\hat{\psi}}{\partial\hat{y}}\frac{\partial\theta}{\partial\hat{x}}-\frac{\partial\hat{\psi}}{\partial\hat{x}}\frac{\partial\theta}{\partial\hat{y}}=\frac{1}{Pe}\left\{\frac{\partial^2\theta}{\partial\hat{x}^2}+\frac{\partial^2\theta}{\partial\hat{y}^2}+N_b\left(\frac{\partial s}{\partial\hat{x}}\frac{\partial\theta}{\partial\hat{x}}+\frac{\partial s}{\partial\hat{y}}\frac{\partial\theta}{\partial\hat{y}}\right)+N_t\left(\left(\frac{\partial\theta}{\partial\hat{x}}\right)^2+\left(\frac{\partial\theta}{\partial\hat{y}}\right)^2\right)\right\} \tag{10}$$

$$\frac{\partial\hat{\psi}}{\partial\hat{y}}\frac{\partial s}{\partial\hat{x}}-\frac{\partial\hat{\psi}}{\partial\hat{x}}\frac{\partial s}{\partial\hat{y}}=\frac{1}{LePe}\left[\left(\frac{\partial^2 s}{\partial\hat{x}^2}+\frac{\partial^2 s}{\partial\hat{y}^2}\right)+\frac{N_t}{N_b}\left(\frac{\partial^2\theta}{\partial\hat{x}^2}+\frac{\partial^2\theta}{\partial\hat{y}^2}\right)\right] \tag{11}$$

where:

$Ra=\frac{(1-\phi_\infty)\rho_{f_\infty}\beta Kg(T_w-T_\infty)l}{\mu\alpha}$ is the Rayleigh number

$Pe=\frac{U_\infty l}{\alpha}$ is the Peclet number

$N_r=\frac{(\rho_p-\rho_{f_\infty})(\phi_w-\phi_\infty)}{\rho_{f_\infty}\beta(T_w-T_\infty)(1-\phi_\infty)}$ is the buoyancy ratio

$N_b=\frac{\gamma D_B(\phi_w-\phi_\infty)}{}$ is the Brownian motion parameter.

$N_t=\frac{\gamma D_T(T_w^\alpha-T_\infty)}{\alpha T_\infty}$ is the thermophoresis parameter and $Le=\alpha/D_B$ is the Lewis number.

We take the following coordinate transformations such that the effect of the wavy surface can be transferred from the boundary conditions into the governing equations:

$$\overline{x}=\hat{x},\quad \overline{y}=(\hat{y}-\delta)Pe^{1/2},\quad \overline{\psi}=Pe^{1/2}\hat{\psi} \tag{12}$$

Substituting Equation (12) into Equations (9)-(11) and letting $Pe\to\infty$ (i.e. boundary layer approximation), we obtain the following boundary layer equations:

$$\left(1+\dot{\delta}^2\right)\frac{\partial^2\overline{\psi}}{\partial\overline{y}^2}=\Delta\left(\sin A+\dot{\delta}\cos A\right)\left(\frac{\partial\theta}{\partial\overline{y}}-N_r\frac{\partial s}{\partial\overline{y}}\right) \tag{13}$$

$$\frac{\partial\overline{\psi}}{\partial\overline{y}}\frac{\partial\theta}{\partial\overline{x}}-\frac{\partial\overline{\psi}}{\partial\overline{x}}\frac{\partial\theta}{\partial\overline{y}}=\left(1+\dot{\delta}^2\right)\left[\frac{\partial^2\theta}{\partial\overline{y}^2}+N_b\frac{\partial s}{\partial\overline{y}}\frac{\partial\theta}{\partial\overline{y}}+N_t\left(\frac{\partial\theta}{\partial\overline{y}}\right)^2\right] \tag{14}$$

$$Le\left(\frac{\partial\overline{\psi}}{\partial\overline{y}}\frac{\partial s}{\partial\overline{x}}-\frac{\partial\overline{\psi}}{\partial\overline{x}}\frac{\partial s}{\partial\overline{y}}\right)=\left(1+\dot{\delta}^2\right)\left(\frac{\partial^2 s}{\partial\overline{y}^2}+\frac{N_t}{N_b}\frac{\partial^2\theta}{\partial\overline{y}^2}\right) \tag{15}$$

where $\Delta=\frac{Ra}{Pe}$ is the mixed convection parameter.

It is obvious from the definition of mixed convection parameter that, as $\Delta \to \infty$ the flow tends to natural convection while the flow tends to forced convection for $\Delta = 0$ and it tends to forced and free convection for $\Delta = 1$. When the values of mixed convection parameter are positive (i.e. Δ is positive), then the buoyancy flow aids the free stream flow and hence the flow is said to be aiding flow and when the buoyancy flow opposes the free stream flow (i.e. Δ is negative), the flow is said to be opposing flow.

Now, we introduce the following similarity transformations to transform the above partial differential equations to ordinary differential equations:

$$\xi = \overline{x}, \quad \eta = \xi^{-1/2}\left(1+\dot{\delta}^2\right)^{-1}\overline{y}, \quad \overline{\psi} = \xi^{1/2} f(\eta) \tag{16}$$

Substituting Equation (16) into Equations (13)-(15), we obtain the following equations:

$$f'' = \Delta\left(\sin A + \dot{\delta}\cos A\right)\left(\theta' - N_r s'\right) \tag{17}$$

$$\theta'' + \frac{1}{2} f\theta' + N_b s'\theta' + N_t \theta'^2 = 0 \tag{18}$$

$$s'' + \frac{1}{2} Lefs' + \frac{N_t}{N_b}\theta'' = 0 \tag{19}$$

The associated boundary conditions are:

$$f = 0, \quad \theta = 1, \quad s = 1, \quad \text{at} \quad \eta = 0 \tag{20a}$$

$$f' \to 1, \quad \theta \to 0, \quad s \to 0 \quad \text{as} \quad \eta \to \infty \tag{20b}$$

Parameters of engineering interest include the study of heat and nanoparticle mass transport problems, namely the Nusselt number Nu_x and nanoparticle Sherwood number NSh_x. These parameters characterize the wall heat and nanoparticle mass transfer rates, respectively.

The local heat and nanoparticle mass fluxes from the wavy plate can be obtained from:

$$q_w = -kn.\nabla T, q_{np} = -D_B n.\nabla\phi \tag{21}$$

where $n = \left(-\dot{\delta}/\sqrt{1+\dot{\delta}^2}, 1/\sqrt{1+\dot{\delta}^2}\right)$ is the unit normal vector to the wavy plate.

The dimensionless local Nusselt number, $Nu_x = xq_w/k(T_w - T_\infty)$ and the nanoparticle Sherwood number $NSh_x = xq_{np}/D_B\left(\phi_w - \phi_\infty\right)$ are given by:

$$\frac{Nu_x}{\sqrt{Pe_x}} = -\sqrt{\frac{1}{1+\dot{\delta}^2}}\left(\frac{\partial\theta}{\partial\eta}\right)_{\eta=0}, \frac{NSh_x}{\sqrt{Pe_x}} = -\sqrt{\frac{1}{1+\dot{\delta}^2}}\left(\frac{\partial s}{\partial\eta}\right)_{\eta=0}, \tag{22}$$

3. Method of solution

Equations (17)-(19) along with the boundary conditions (20) were solved using the numerical method namely, SLM (Motsa and Shateyi, 2006; Makukula *et al.*, 2010;

Awad *et al.*, 2011). In this method the independent variables $f(\eta)$, $\theta(\eta)$ and s(η) are assumed to be expressed as:

$$f(\eta) = f_i(\eta) + \sum_{n=0}^{i-1} f_n(\eta), \quad \theta(\eta) = \theta_i(\eta) + \sum_{n=0}^{i-1} \theta_n(\eta), \quad s(\eta) = s_i(\eta) + \sum_{n=0}^{i-1} s_n(\eta) \tag{23}$$

where f_i, θ_i and s_i ($i = 1, 2, 3, \ldots$), are unknown functions and f_n, θ_n and s_n are the approximations which are obtained by recursively solving the linear part of the equation system that results from substituting Equation (23) in Equations (17)-(19).

The initial guesses $f_0(\eta)$, $\theta_0(\eta)$ and $s_0(\eta)$ are taken as:

$$f_0(\eta) = 1 + \eta - e^{-\eta}, \quad \theta_0(\eta) = e^{-\eta}, \quad s_0(\eta) = e^{-\eta} \tag{24}$$

These initial approximations are chosen such that they satisfy the boundary conditions (20). The subsequent solutions f_i, θ_i, s_i, $i \geqslant 1$ are obtained by successively solving the linearized form of the equations which are obtained by substituting Equation (23) in the governing equations and neglecting the non-linear terms. The linearized equations to be solved are:

$$f_i'' + a_{1,i-1}\theta_i' + a_{2,i-1}s_i' = r_{1,i-1} \tag{25}$$

$$\theta_i'' + b_{1,i-1}\theta_i' + b_{2,i-1}s_i' + b_{3,i-1}f_i = r_{2,i-1} \tag{26}$$

$$s_i'' + c_{1,i-1}s_i' + c_{2,i-1}\theta_i'' + c_{3,i-1}f_i = r_{3,i-1} \tag{27}$$

where:

$$a_{1,i-1} = -\Delta(\sin A + \dot{\delta}\cos A), \quad a_{2,i-1} = N_r\Delta(\sin A + \dot{\delta}\cos A) \tag{28}$$

$$b_{1,i-1} = \frac{1}{2}\sum_{n=0}^{i-1} f_n + N_b\sum_{n=0}^{i-1} s_n' + 2N_t\sum_{n=0}^{i-1}\theta_n', \quad b_{2,i-1} = N_b\sum_{n=0}^{i-1}\theta_n', \quad b_{3,i-1} = \frac{1}{2}\sum_{n=0}^{i-1}\theta_n'$$

$$c_{1,i-1} = \frac{1}{2}Le\sum_{n=0}^{i-1} f_n, \quad c_{2,i-1} = \frac{N_t}{N_b}, \quad c_{3,i-1} = \frac{1}{2}Le\sum_{n=0}^{i-1} s_n'$$

$$r_{1,i-1} = -\sum_{n=0}^{i-1} f_n'' + \Delta(\sin A + \dot{\delta}\cos A)\sum_{n=0}^{i-1}\theta_n' - \Delta(\sin A + \dot{\delta}\cos A)N_r\sum_{n=0}^{i-1} s_n'$$

$$r_{2,i-1} = -\sum_{n=0}^{i-1}\theta_n'' - \frac{1}{2}\sum_{n=0}^{i-1} f_n\sum_{n=0}^{i-1}\theta_n' - N_b\sum_{n=0}^{i-1} s_n'\sum_{n=0}^{i-1}\theta_n' - N_t\sum_{n=0}^{i-1}\theta_n'\sum_{n=0}^{i-1}\theta_n'$$

$$r_{3,i-1} = -\sum_{n=0}^{i-1} s_n'' - \frac{1}{2}\sum_{n=0}^{i-1} f_n\sum_{n=0}^{i-1} s_n' - \frac{N_t}{N_b}\sum_{n=0}^{i-1}\theta_n''$$

The boundary conditions reduce to:

$$f_i(0) = f_i^{'}(\infty) = 0, \theta_i(0) = \theta_i(\infty) = s_i(0) = s_i(\infty) = 0 \tag{29}$$

The solutions f_i, θ_i, s_i ($i \geqslant 1$) are obtained by iteratively solving Equations (25)-(27). The approximate solutions for $f(\eta)$, $\theta(\eta)$ and $s(\eta)$ are then obtained as:

$$f(\eta) \approx \sum_{m=0}^{M} f_m(\eta), \quad \theta(\eta) \approx \sum_{m=0}^{M} \theta_m(\eta), \quad s(\eta) \approx \sum_{m=0}^{M} s_m(\eta) \tag{30}$$

where M is the order of SLM approximation. Equations (25)-(27) were solved using the Chebyshev spectral collocation method (Canuto *et al.*, 1988). The unknown functions are approximated by the Chebyshev interpolating polynomials in such a way that they are collocated at the Gauss-Lobatto points defined as:

$$\xi_j = \cos\frac{\pi j}{N}, \quad j = 0, 1, 2, ..., N \tag{31}$$

where N is the number of collocation points used. The physical region $[0,\infty)$ is transformed into the region $[-1, 1]$ using the domain truncation technique in which the problem is solved on the interval [0, L] instead of [0, ∞). This leads to the mapping:

$$\frac{\eta}{L} = \frac{\xi + 1}{2}, \quad -1 \leqslant \xi \leqslant 1 \tag{32}$$

where L is a scaling parameter used to invoke the boundary condition at infinity. The functions f_i, θ_i and s_i are approximated at the collocation points by:

$$f_i(\xi) = \sum_{k=0}^{N} f_i(\xi_k) T_k(\xi_j), \ \theta_i(\xi) = \sum_{k=0}^{N} \theta_i(\xi_k) T_k(\xi_j), \ s_i(\xi) = \sum_{k=0}^{N} s_i(\xi_k) T_k(\xi_j),$$

$$j = 0, 1, 2, ..., N \tag{33}$$

where T_k is the kth Chebyshev polynomial defined by:

$$T_k(\xi) = \cos\left[k \cos^{-1}\xi\right] \tag{34}$$

The derivatives of the variables at the collocation points are represented as:

$$\frac{d^a f_i}{d\eta^a} = \sum_{k=0}^{N} \mathbf{D}_{kj}^a f_i(\xi_k), \ \frac{d^a \theta_i}{d\eta^a} = \sum_{k=0}^{N} \mathbf{D}_{kj}^a \theta_i(\xi_k), \ \frac{d^a s_i}{d\eta^a} = \sum_{k=0}^{N} \mathbf{D}_{kj}^a s_i(\xi_k),$$

$$j = 0, 1, 2, ..., N. \tag{35}$$

where a is the order of differentiation and $\mathbf{D} = \frac{2}{L}\mathcal{D}$ with D being the Chebyshev spectral differentiation matrix.

Substituting Equations (32)-(35) into Equations (25)-(27) leads to the matrix equation:

$$\mathbf{A}_{i-1}\mathbf{X}_i = \mathbf{R}_{i-1}, \tag{36}$$

subject to the boundary conditions:

$$f_i(\xi_N) = 0, \quad \sum_{k=0}^{N} \mathbf{D}_{0k} f_i(\xi_k) = 0 \tag{37}$$

$$\theta_i(\xi_N) = \theta_i(\xi_0) = s_i(\xi_N) = s_i(\xi_0) = 0 \tag{38}$$

In Equation (35) $\mathbf{A}_{i-1}$ is a $(3N+3)\times(3N+3)$ square matrix and $\mathbf{X}_i$ and $\mathbf{R}_{i-1}$ are $(3N+3)\times 1$ column vectors defined by:

$$\mathbf{A}_{i-1} = \begin{bmatrix} A_{11} & A_{12} & A_{13} \\ A_{21} & A_{22} & A_{23} \\ A_{31} & A_{32} & A_{33} \end{bmatrix}, \quad \mathbf{X}_i = \begin{bmatrix} \mathbf{F}_i \\ \Theta_i \\ \Phi_i \end{bmatrix}, \quad \mathbf{R}_{i-1} = \begin{bmatrix} \mathbf{r}_{1,i-1} \\ \mathbf{r}_{2,i-1} \\ \mathbf{r}_{3,i-1} \end{bmatrix} \tag{39}$$

where:

$$\mathbf{F}_i = [f_i(\xi_0), f_i(\xi_1), \ldots\ldots, f_i(\xi_{N-1}), f_i(\xi_N)]^T, \tag{40}$$

$$\Theta_i = [\theta_i(\xi_0), \theta_i(\xi_1), \ldots\ldots, \theta_i(\xi_{N-1}), \theta_i(\xi_N)]^T,$$

$$\Phi_i = [s_i(\xi_0), s_i(\xi_1), \ldots\ldots, s_i(\xi_{N-1}), s_i(\xi_N)]^T,$$

$$\mathbf{r}_{1,i-1} = \left[r_{1,i-1}(\xi_0), r_{1,i-1}(\xi_1), \ldots\ldots, r_{1,i-1}(\xi_{N-1}), r_{1,i-1}(\xi_N)\right]^T$$

$$\mathbf{r}_{2,i-1} = \left[r_{2,i-1}(\xi_0), r_{2,i-1}(\xi_1), \ldots\ldots, r_{2,i-1}(\xi_{N-1}), r_{2,i-1}(\xi_N)\right]^T$$

$$\mathbf{r}_{3,i-1} = \left[r_{3,i-1}(\xi_0), r_{3,i-1}(\xi_1), \ldots\ldots, r_{3,i-1}(\xi_{N-1}), r_{3,i-1}(\xi_N)\right]^T$$

$$A_{11} = \mathbf{D}^2, \quad A_{12} = a_{1,i-1}\mathbf{D}, \quad A_{13} = a_{2,i-1}\mathbf{D}$$

$$A_{21} = b_{3,i-1}I, \quad A_{22} = \mathbf{D}^2 + b_{1,i-1}\mathbf{D}, \quad A_{23} = b_{2,i-1}\mathbf{D}$$

$$A_{31} = c_{3,i-1}I, \quad A_{32} = c_{2,i-1}\mathbf{D}^2, \quad A_{33} = \mathbf{D}^2 + c_{1,i-1}\mathbf{D}$$

Here $a_{k,i-1}$, $b_{l,i-1}$, $c_{l,i-1}$ ($k = 1, 2$) and ($l = 1, 2, 3$) are diagonal matrices of size $(N+1)\times(N+1)$ and I is an identity matrix of size $(N+1)\times(N+1)$. After modifying the matrix system (36) to incorporate boundary conditions (37)-(38), the solution is obtained as:

$$\mathbf{X}_i = \mathbf{A}_{i-1}^{-1}\mathbf{R}_{i-1} \tag{41}$$

4. Results and discussions

Solutions for the dimensionless velocity, temperature and nanoparticle volume fraction functions and heat and nanoparticle mass transfer rates for aiding and opposing flows

have been computed and displayed graphically in Figures (2)-(9). The effects of angle of inclination A, Brownian motion parameter (N_b), thermophoresis parameter N_t and amplitude a of the wave surface for both aiding and opposing flows have been discussed.

Tables (I) and (II) show the comparison of the results of the present paper for both aiding and opposing flows for fixed values of $A = \pi/2$, $a = 0$, $\xi = 0$, $N_r = 0$, $N_t = 0$, $N_b = 0.001$, $Le = 0$ with the results obtained by P. Cheng (1977). It is shown that these two results are in excellent agreement.

Tables (III) and (IV) gives the comparison of the result of Nusselt and nanoparticle Sherwood numbers for fixed values of $N_b = 0.5$, $Nt = 0.1$, $\Delta = 1.0$, $Le = 5.0$, $N_r = 0.3$ with varying amplitude and angle of inclination of the wavy surface respectively by SLM with Shooting method. We observe that in both of these tables, increasing the amplitude of the wave surface decreases the heat and nanoparticle mass transfer rates

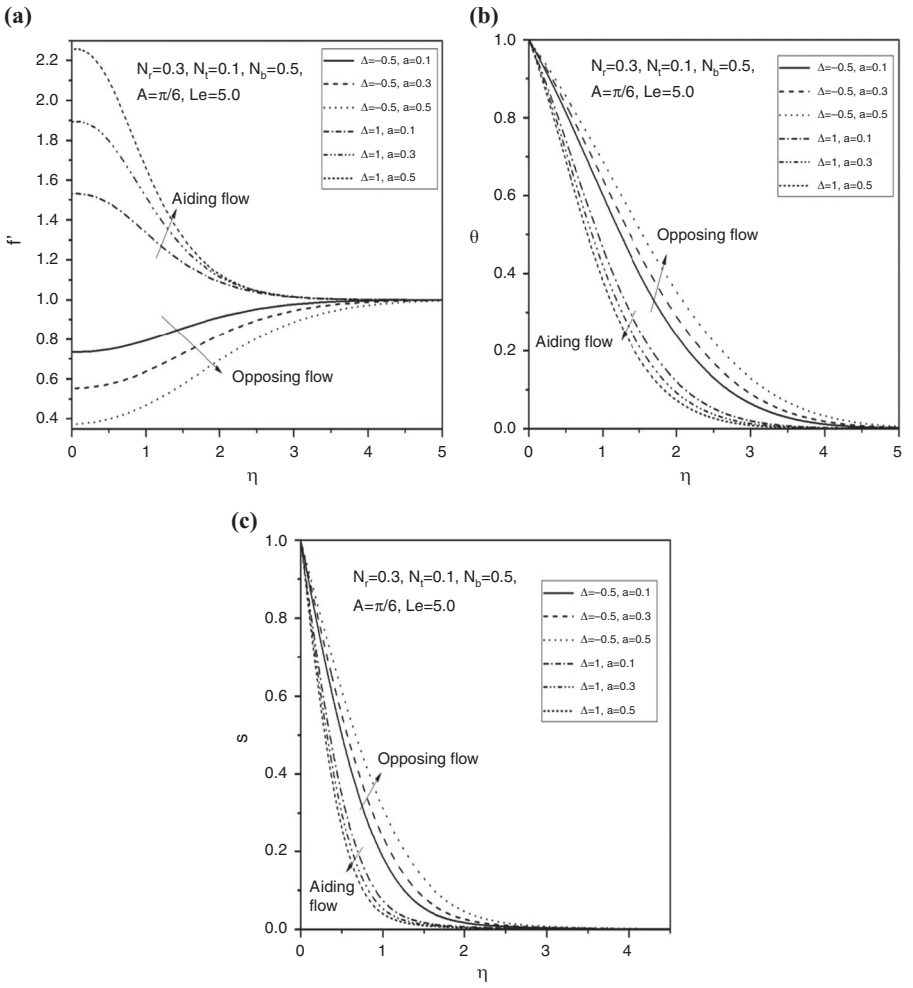

Figure 2.
Variation of (a) velocity, (b) temperature, (c) nanoparticle volume fraction profiles with the wave amplitude (a)

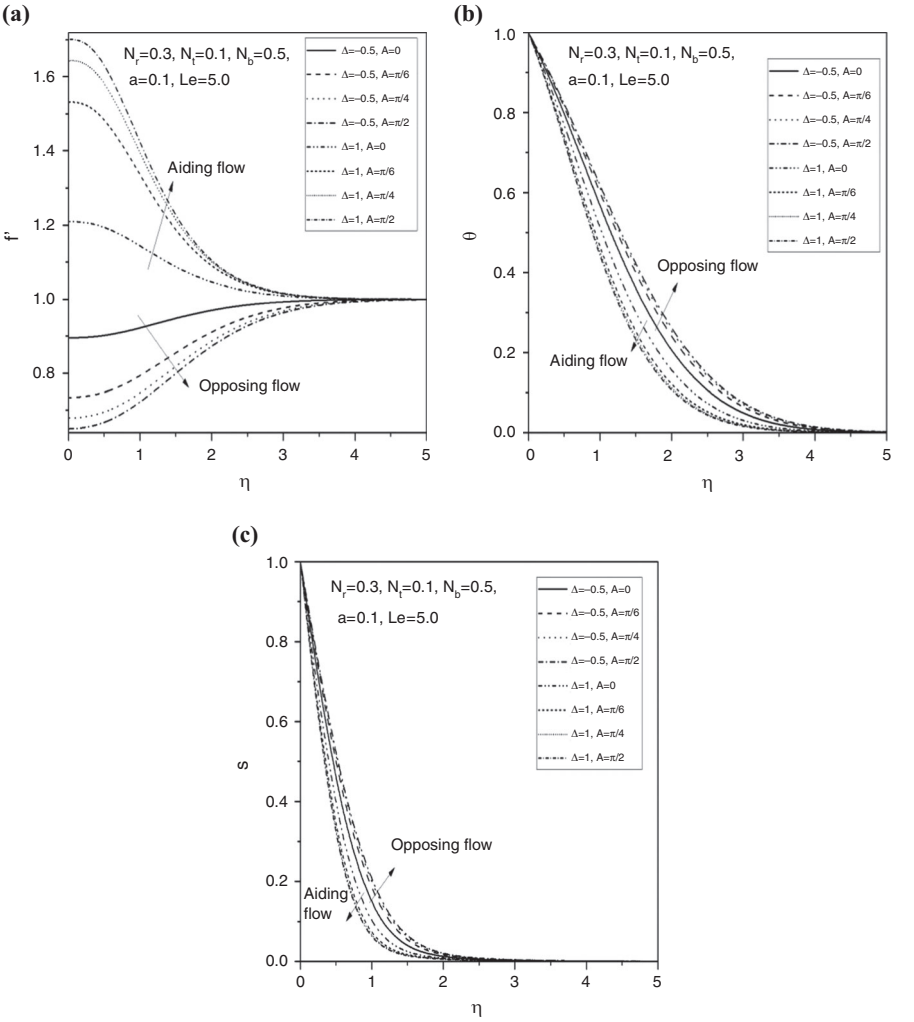

Figure 3.
Variation of (a) velocity, (b) temperature, (c) nanoparticle volume fraction profiles with angle of inclination (A)

and increasing the angle of inclination of the wavy surface to the horizontal enhances the heat and nanoparticle mass transfer rates. We also notice that in both the tables, the SLM converges rapidly to a fixed value in less number of iterations. We also calculated these values by using Shooting method. Hence both the results obtained by SLM and Shooting method are found to be same.

Figure 2(a)-(c) shows the effect of the amplitude of the wavy surface on velocity, temperature and nanoparticle volume fraction distributions. It is observed that as a increases, velocity increases near the plate and decreases away from the plate in the case of aiding flow while in the case of opposing flow, velocity decreases near the plate and increases away from the plate. But the temperature and nanoparticle volume fraction decreases for aiding flow and increases for opposing flow.

The effect of the angle of inclination of the wavy surface on velocity, temperature and nanoparticle volume fraction is plotted in Figure 3(a)-(c). The similarity equations

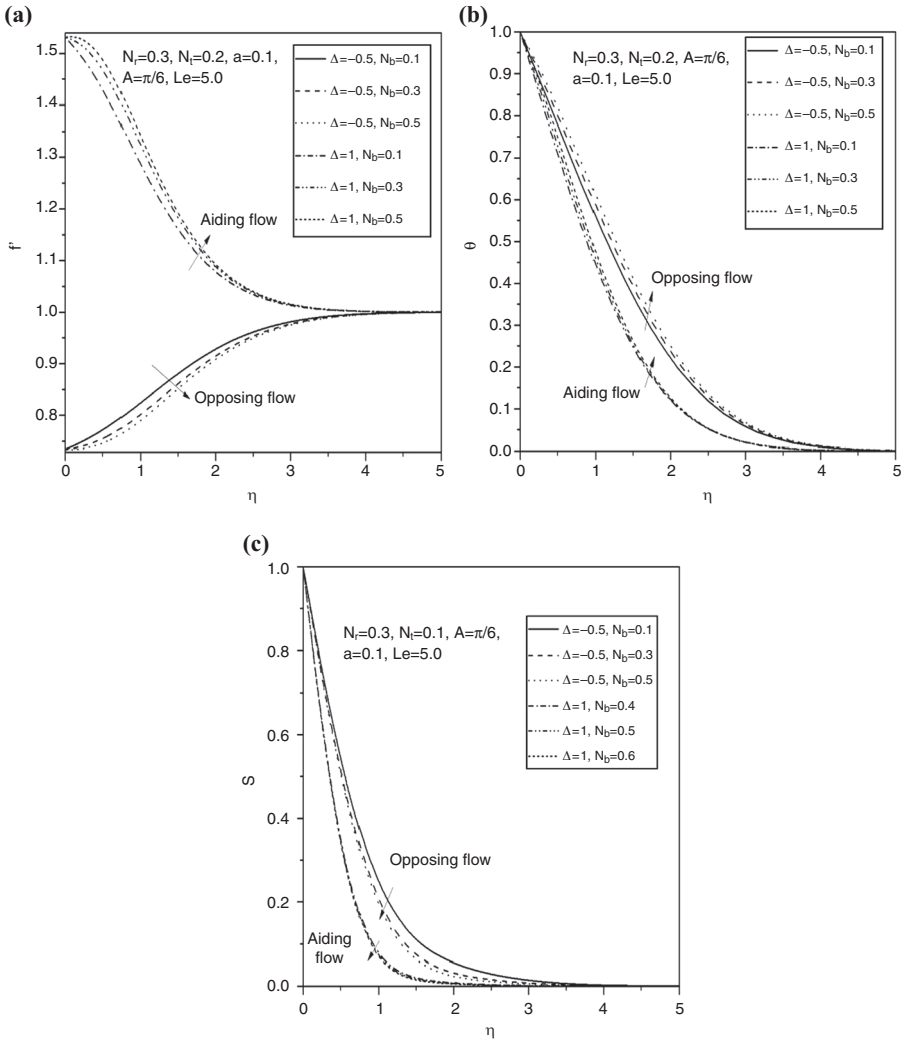

Figure 4.
Variation of (a) velocity, (b) temperature (c) nanoparticle volume fraction profiles with Brownian motion parameter (N_b)

for the limiting cases of the horizontal and vertical plates are recovered from the transformed equations by setting $A = 0°$ and $A = 90°$, respectively. It is noted from Figure 3(a)-(c) that as A increases, the velocity increases near the plate and decreases away from the plate for aiding flow whereas the velocity decreases near the plate and increases away from the plate for opposing flow. But the temperature and nanoparticle volume fraction decrease within the boundary layer region for the aiding flow and increases for opposing flow. When the surface is vertical, the smallest temperature and nanoparticle volume fraction distributions are observed for aiding flow whereas largest temperature and nanoparticle volume fraction distributions are observed for opposing flow. While for the horizontal surface, largest temperature and nanoparticle volume fraction distributions are observed for aiding flow whereas smallest temperature and nanoparticle volume fraction distributions are observed for opposing flow.

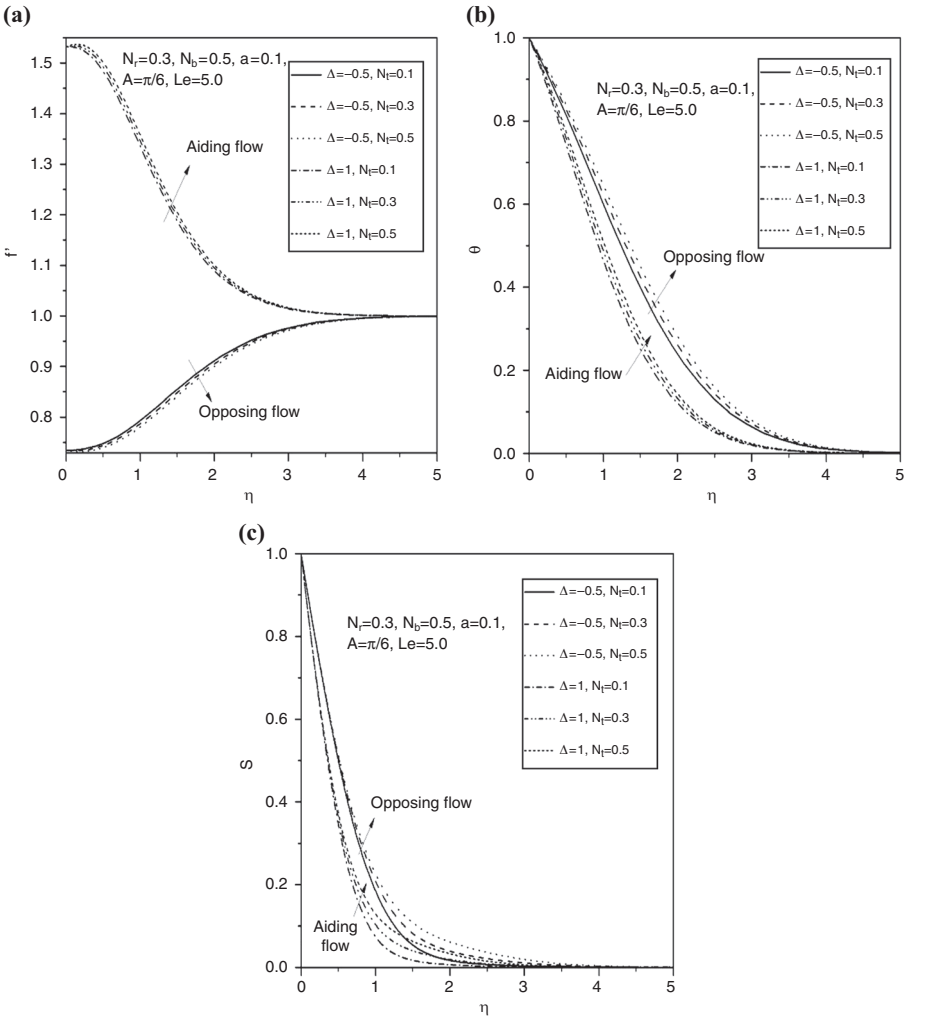

Figure 5.
Variation of (a) velocity, (b) temperature (c) nanoparticle volume fraction profiles with thermophoresis parameter (N_t)

Figures 4 and 5 shows the distributions of the dimensionless velocity component, temperature and nanoparticle fraction for different values of Brownian motion parameter N_b and thermophoresis parameter N_t. It is observed that an increase in the intensity of Brownian motion parameter produces an enhancement in the fluid velocity within the momentum boundary layer thus enhancing the fluid flow in the case of aiding flow whereas in the case of opposing flow the velocity of the fluid flow decreases, as shown in Figure 4(a). Figure 5(a) depicts that an increase in the thermophoresis parameter tends to increase the maximum stream wise velocity, thus assisting the fluid flow in the case of aiding flow, while in the case of opposing flow, the velocity of the fluid flow decreases. Figure 4(b) shows that as the Brownian motion parameter increases, the temperature of the fluid in the boundary layer increases for both aiding and opposing flows. Moreover, the temperature increases in both the cases (i.e. Aiding and opposing flow) with an increase in the thermophoresis parameter,

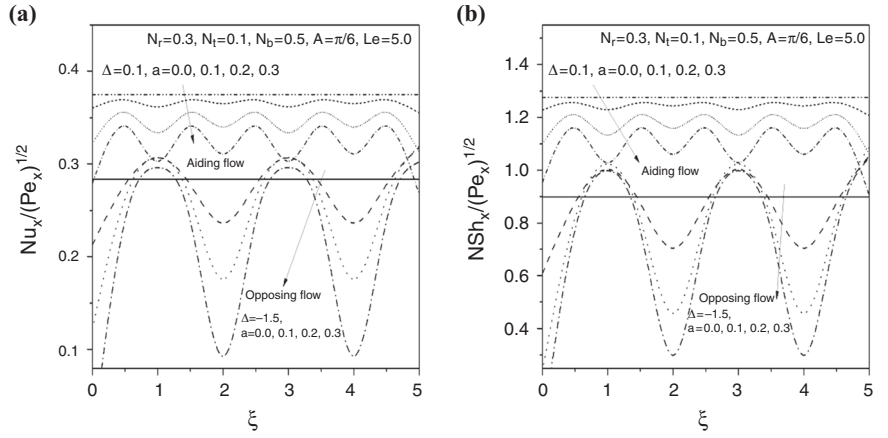

Figure 6.
Effect of the wave amplitude a on the heat and nanoparticle mass transfer rates

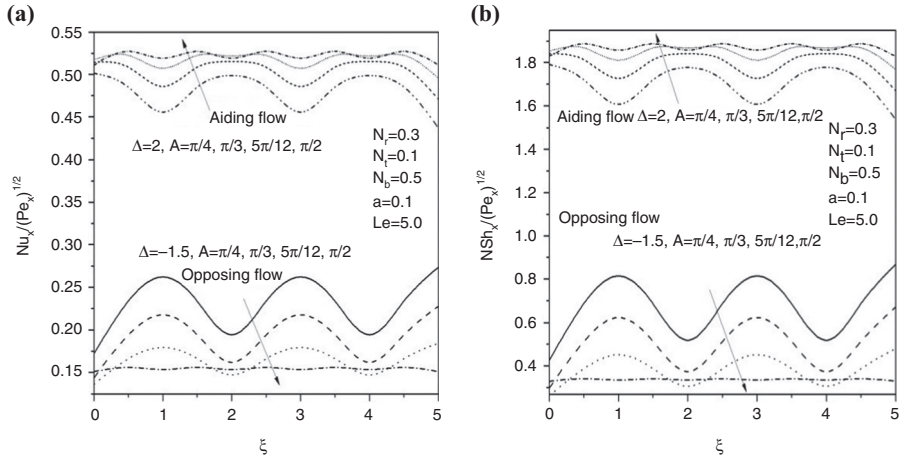

Figure 7.
Effect of the angle of inclination (A) on the heat and nanoparticle mass transfer rates

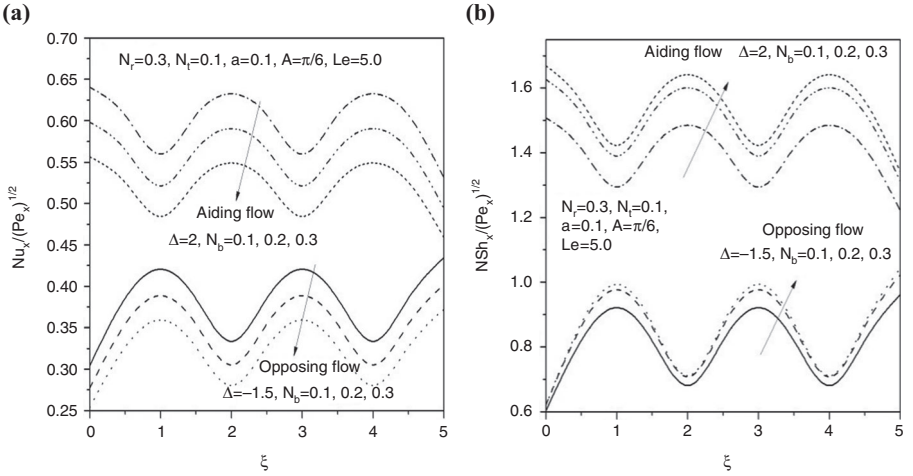

Figure 8.
Effect of the Brownian motion parameter (N_b) on the heat and nanoparticle mass transfer rates

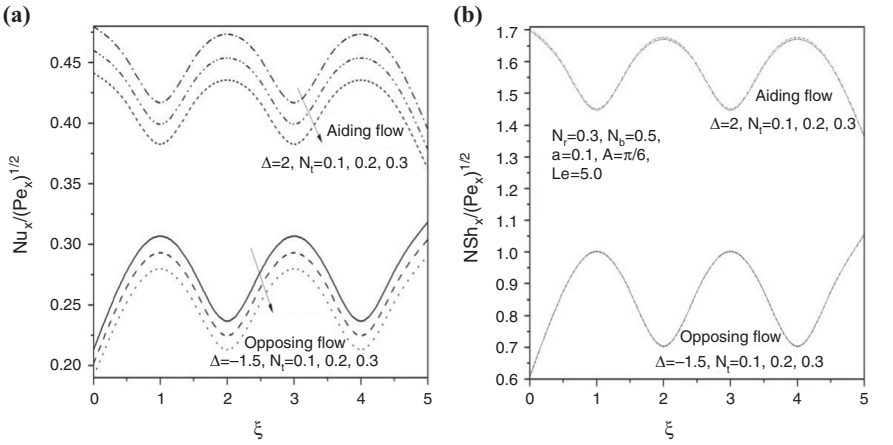

Figure 9.
Effect of the thermophoresis parameter (N_t) on the heat and nanoparticle mass transfer rates

Table I.
Comparison of $-\theta'(0)$ for Aiding flow by the present method and Cheng (1977) for fixed values of $A = \pi/2$, a = 0, $\xi = 0$, $N_r = 0$, $N_t = 0$, $N_b = 0.001$, Le = 0

Δ	$-\theta'(0)$ Cheng (1977)	Present
0	0.5641	0.56416137
0.5	0.6473	0.64736502
1	0.7205	0.72055074
3	0.9574	0.9574317
10	1.516	1.51620246
20	2.066	2.066

Table II.
Comparison of $-\theta'(0)$ for Opposing flow by the present method and Cheng (1977) for fixed values of $A=\pi/2$, a=0, $\xi=0$, $N_r=0$, $N_t=0$, $N_b=0.001$, Le=0

Δ	$-\theta'(0)$ Cheng (1977)	Present
−0.2	0.5269	0.52691622
−0.4	0.4865	0.48654006
−0.6	0.442	0.4423002
−0.8	0.3916	0.39167494
−1.0	0.332	0.3323673

as shown in Figure 5(b). Increasing the Brownian motion parameter tends to reduce the nanoparticle volume fraction for both aiding and opposing flows as shown in Figure 4(c). However, the reverse trend is observed in case of thermophoresis parameter, i.e. an increase in the value of the thermophoresis parameter enhances the nanoparticle volume fraction for both aiding and opposing flows as shown in Figure 5(c).

Figure 6(a)-(b) show the effect of the wave amplitude on the Nusselt and the nanoparticle Sherwood number. This figure reveals that an enhancement in wave amplitude causes small fluctuations in the heat and nanoparticle transfer rates for both aiding and opposing flows. In general, we conclude that the surface becomes more roughened for increasing values of amplitude of the wave surface.

The variation of heat and nanoparticle mass transfer rates for various values of the angle of inclination A is displayed in Figure 7 (a)-(b). This figure shows that increasing the angle of inclination increases the buoyancy force and assists the flow, leading to an increase in the heat and nanoparticle mass transfer rates for aiding flow while the reverse trend is observed in opposing flow.

The effect of Brownian motion parameter N_b on the heat and nanoparticle mass transfer rates is presented in Figure 8. Figure 8(a) depicts that for both aiding and opposing flows, the dimensionless heat transfer rate decreases with the increase in the Brownian motion parameter and an increase in the value of the Brownian motion parameter enhances the nanoparticle mass transfer rate, as shown in Figure 8(b).

Figure 9 depicts the streamwise distribution of Nusselt and Sherwood numbers for different values of thermophoresis parameter. It is seen from Figure 9(a) that for both aiding and opposing flows, the heat transfer rate decreases with the increase in the thermophoresis parameter. The effect of thermophoresis number on the nanoparticle mass transfer is negligible on the nanoparticle Sherwood number as depicted in Figure 9(b).

Brownian motion is proportional to the volumetric of nanoparticles in the direction from high to low concentration, whereas the thermophoresis is proportional to the temperature gradient from hot to cold. Hence, we conclude that the effect of the combination of Brownian motion and thermophoresis is to reduce the value of Nusselt number. Increasing the buoyancy ratio parameter N_r decreases both the local Nusselt and local nanoparticle Sherwood number. This is due to the presence of buoyancy force in the flow region which gives large temperature and concentration resulting in the decay of heat and nanoparticle mass transfer rate.

The Lewis number is an important parameter in heat and mass transfer processes as it gives the ratio of thicknesses of the thermal and concentration boundary layers.

Table III. comparison of values of the $Nu_x/\sqrt{Pe_x}$ and $NSh_x/\sqrt{Pe_x}$ for $\Delta = 1.0$, Le = 5.0, $N_r = 0.3$, $N_t = 0.1$, $N_b = 0.5$, A = π/6 at different orders of SLM approximation with Shooting method

		SLM					
	a	Order 2	Order 3	Order 4	Order 6	Order 8	Shooting method
$\frac{Nu_x}{\sqrt{Pe_x}}$	0.3	0.3513021	0.3591137	0.359184	0.359184	0.359184	0.3592
	0.6	0.2538827	0.2624982	0.2626787	0.2626787	0.2626787	0.2627
	0.9	0.196856	0.2055278	0.2058451	0.2058451	0.2058451	0.2058
$\frac{NSh_x}{\sqrt{Pe_x}}$	0.3	1.2982403	1.2709696	1.2707575	1.2707575	1.2707575	1.2708
	0.6	0.9856430	0.9416141	0.9407770	0.9407770	0.9407770	0.9408
	0.9	0.8016100	0.7452722	0.7433358	0.7433358	0.7433358	0.7433

Table IV. Comparision of values of the $Nu_x/\sqrt{Pe_x}$ and $NSh_x/\sqrt{Pe_x}$ for $\Delta = 1.0$, Le = 5.0, $N_r = 0.3$, $N_t = 0.1$, $N_b = 0.5$, a = 0.1 at different orders of SLM approximation with Shooting method

		SLM					
	A	Order 2	Order 3	Order 4	Order 6	Order 8	Shooting method
$\frac{Nu_x}{\sqrt{Pe_x}}$	π/6	0.4161041	0.4218821	0.4219026	0.4219026	0.4219026	0.4219
	π/4	0.4276493	0.4346912	0.4347263	0.4347263	0.4347263	0.4347
	π/3	0.4344536	0.4422910	0.4423378	0.4423378	0.4423378	0.4423
$\frac{NSh_x}{\sqrt{Pe_x}}$	π/6	1.4879164	1.4747014	1.4746631	1.4746631	1.4746631	1.4747
	π/4	1.544790	1.5259824	1.5259042	1.5259042	1.5259042	1.5259
	π/3	1.5790825	1.5563666	1.5562523	1.5562523	1.5562523	1.5563

The effect of Lewis number on the concentration has similarities to the Prandtl number effect on the temperature. Therefore, increasing the Lewis number tends to decrease the concentration boundary layer thickness, thus increasing the mass transfer rate between the porous medium and the surface.

5. Conclusion

(1) An increase in the Brownian motion parameter N_b, increases the velocity, temperature and local nanoparticle mass transfer coefficient for aiding flow, but reduces the nanoparticle volume fraction and local heat transfer coefficient for both aiding and opposing flows.

(2) A higher value of the thermophoresis parameter N_t leads to higher temperatures and nanoparticle volume fraction for both aiding and opposing flows, but an increase in velocity for aiding flow and decrease in velocity for opposing flow is observed. Moreover, lower local heat transfer coefficient for both aiding and opposing flows and no effect on the mass transfer coefficient is observed.

(3) The effect of the amplitude of the wavy surface is to increase the velocity, temperature, nanoparticle volume fraction of aiding flow and the reverse trend is observed for opposing flow. The local heat transfer coefficient and local nanoparticle mass transfer coefficient reduces for both aiding and opposing flows.

(4) The influence of the angle of inclination of the wavy surface to the horizontal is to enhance the velocity, temperature, nanoparticle volume fraction, the local heat transfer and nanoparticle mass transfer coefficients for aiding flow and the reverse trend is observed in opposing flow.

References

Ahmad, S. and Pop, I. (2010), "Mixed convection boundary layer flow from a vertical flat plate embedded in a porous medium filled with nanofluids", *International Communications in Heat Mass Transfer*, Vol. 37 No. 8, pp. 987-991.

Awad, F.G., Sibanda, P., Motsa, S.S. and Makinde, O.D. (2011), "Convection from an inverted cone in a porous medium with cross-diffusion effects", *Computers and Mathematics with Applications* Vol. 61 No. 5, pp. 1431-1441.

Buongiorno, J. (2006), "Convective transport in nanofluids", *Journal of Heat Transfer*, Vol. 128 No. 3, pp. 240-250.

Canuto, C., Hussaini, M.Y., Quarteroni, A. and Zang, T.A. (1988), *Spectral Methods in Fluid Dynamics*, Springer-Verlag, Berlin.

Chamkha, A.J., Rashad, M. and Gorla, R.S.R. (2014), "Non-similar solutions for mixed convection along a wedge embedded in a porous medium saturated by a non-newtonian nanofluid: natural convection dominated regime", *International Journal of Numerical Methods for Heat & Fluid Flow*, Vol. 24 No. 7, pp. 1471-1486.

Chamkha, A.J., Abbasbandy, S., Rashad, A.M. and Vajravelu, K. (2013), "Radiation effect on mixed convection about a cone embedded in a porous medium filled with a nanofluid", *Meccanica*, Vol. 48 No. 2, pp. 275-285.

Cheng, P. (1977), "Combined free and forced convection flow about inclined surfaces in porous media", *International Journal of Heat Mass Transfer*, Vol. 20 No. 8, pp. 807-814.

Cheng, P. and Minkowycz, W.J. (1977), "Free convection about a vertical flat plate embedded in a porous medium with application to heat transfer from a dike", *Journal of Geophysical Research*, Vol. 82 No. 14, pp. 2040-2044.

Chin, K.E., Nazar, R., Arifin, N.M. and Pop, I. (2007), "Effect of variable viscosity on mixed convection boundary layer flow over a vertical surface embedded in a porous medium", *International Communications in Heat Mass Transfer*, Vol. 34 No. 4, pp. 464-473.

Choi, S.U.S. (1995), "Enhancing thermal conductivity of fluids with nanoparticles", *Developments and Applications of Non-Newtonian Flows*, Vol. 66, pp. 99-105.

Das, S.K., Choi, S.U.S., Yu, W. and Pradeep, T. (2007), *Nanofluids: Science and Technology*, Wiley.

Gorla, R.S.R. and Hossain, A. (2013), "Mixed convective boundary layer flow over a vertical cylinder embedded in a porous medium saturated with a nanofluid", *International Journal of Numerical Methods for Heat & Fluid Flow*, Vol. 23 No. 8, pp. 1393-1405.

Guerroudj, N. and Kahalerras, H. (2012), "Mixed convection in an inclined channel with heated porous blocks", *International Journal of Numerical Methods for Heat & Fluid Flow*, Vol. 22 No. 7, pp. 839-861.

Hang, X., Tao, F. and Pop, I. (2013), "Analysis of mixed convection flow of a nanofluid in a vertical channel with the Buongiorno mathematical model", *International Communications in Heat Mass Transfer*, Vol. 44, pp. 15-22.

Hsu, P.-T., Taiwan, K., Chen, C.-K., Wang, C.-C. and Taiwan, T. (2000), "Mixed convection of micropolar fluids along a vertical wavy surface", *Acta Mechanica*, Vol. 144 No. 3, pp. 231-247.

Ingham, D.B. and Pop, I. (Eds), (2005), *Transport Phenomena in Porous Media*, Vol. 3, Elsevier, Oxford.

Jang, J.-H. and Yan, W.-M. (2004), "Mixed convection heat and mass transfer along a vertical wavy surface", *International Journal of Heat Mass Transfer*, Vol. 47 No. 3, pp. 419-428.

Kakac, S. and Pramuanjaroenkij, A. (2009), "Review of convective heat transfer enhancement with nanofluids", *International Journal of Heat and Mass Transfer*, Vol. 52 Nos 13-14, pp. 3187-3196.

Lai, F.C. (1991), "Coupled heat and mass transfer by mixed convection from a vertical plate in a saturated porous medium", *International Communications in Heat Mass Transfer*, Vol. 18 No. 1, pp. 93-106.

Makukula, Z.G., Sibanda, P. and Motsa, S.S. (2010), "A novel numerical technique for two dimensional laminar flow between two moving porous walls", *Mathematical Problems in Engineering*, Vol. 2010, Article ID 528956, p. 15.

Merkin, J.H. (1980), "Free convetion boundary layer flow on a vertical surface in a saturated porous medium", *Journal of Engineering Mathematics*, Vol. 14 No. 4, pp. 301-303.

Molla, M.M. and Hossain, M.A. (2007), "Radiation effect on mixed convection laminar flow along a vertical wavy surface", *International Journal of Thermal Sciences*, Vol. 46 No. 9, pp. 926-935.

Motsa, S.S. and Shateyi, S. (2006), "Successive linearisation solution of free convection non-darcy flow with heat and mass transfer", *Advanced Topics in Mass Transfer*, Vol. 19, pp. 425-438.

Moulic, S.G. and Yao, L.S. (1989), "Mixed convection along a wavy surface", *Journal of Heat Transfer*, Vol. 111 No. 4, pp. 974-979.

Nield, D.A. and Bejan, A. (2006), *Convection in Porous Media*, 4th ed., Springer.

Nitesh, M., Manoj, V., Santosh Kumar, D. and Satheesh, A. (2013), "Numerical simulation of mixed convection in a porous medium filled with water/Al_2O_3 nanofluid", *Heat Transfer-Asian Research*, Vol. 42 No. 1, pp. 1-14.

Rohni, A.M., Ahmad, S., Merkin, J.H. and Pop, I. (2013), "Mixed convection boundary layer flow along a vertical cylinder embedded in a porous medium filled by a nanofluid", *Transport in Porous Media*, Vol. 96 No. 2, pp. 237-253.

Roşca, N.C., Roşca, A.V., Groşan, T. and Pop, I. (2014), "Mixed convection boundary layer flow past a vertical flat plate embedded in a non-Darcy porous medium saturated by a nanofluid", *International Journal of Numerical Methods for Heat & Fluid Flow*, Vol. 24 No. 5, pp. 970-987.

Vafai, K. (Ed.), (2005), *Handbook of Porous Media*, 2nd ed., *Taylor and Francis*, NY.

Wang, C.-C. and Chen, C.'o.-K. (2005), "Mixed convection boundary layer flow on inclined wavy plates including the magnetic field effect", *International Journal of Thermal Sciences*, Vol. 44 No. 6, pp. 577-586.

Xuan, Y.M. and Li, Q. (2000), "Heat transfer enhancement of nanofluids", *International Journal of Heat and Fluid Flow*, Vol. 21 No. 1, pp. 58-64.

Corresponding author
Dr D. Srinivasacharya can be contacted at: dsrinivasacharya@yahoo.com